International Journal of Innovations in Engineering and Technology (IJIET)
http://dx.doi.org/10.21172/ijiet.143.11

Microneedles – A New Era Of Drug Delivery System

Sanjesh kumar[1], Mansi singh[2]
[1,2]*Department of pharmacy,Lotus institute of pharmacy,Bareilly, Bareilly(U.P.) India*

Abstract- Micro-needle (MN), a kind of micro-device, has been projected to act as drug delivery systems since 1990s. It can be made from silicon, metal, polymer and ceramic materials. Many promising therapeutic agents are limited by their inability to reach the systemic circulation, due to the excellent barrier properties of biological membranes, such as the stratum corneum (SC) of the skin or the sclera/cornea of the eye and others. The outermost layer of the skin, the SC, is the principal barrier to topically-applied medications. A broad range of biopharmaceuticals are delivered by MN into skin, especially the supra-molecule which cannot get through the stratum corneum. MN causes less pain and increases drug absorption by orders of magnitude compared to hypodermic syringe. Several published articles in a decade have been reported, demonstrating a great progress in the design, manufacture and application of MN. This review glimpses on the fabrication materials of MN, preparation methods and delivery applications of MN in human diseases. Potential safety aspects in these transdermal drug delivery systems are also described in detail.
Keywords micro-needle, etching, transdermal drug delivery, biopharmaceuticals, stratum corneum

I. INTRODUCTION

MICRONEEDLES

Microneedles (MN) consist of a plurality of microprojections, generally 25 to 2,000 μm in height, of different shapes, which are attached to a base support. The application of MN matrices on biological membranes can create micron transport pathways (1). Once created, these micropores or pathways have orders of magnitude greater than the molecular dimensions and should therefore easily allow the transport of macromolecules, as well as possibly complexes and microparticles supramolecular (2). In addition, MNs could also be used to take samples of body fluids, for example to measure blood glucose levels in the treatment of diabetes. ALZA appears to be the first to design MN, described in a 1976 patent (3). However, the manufacture of such microstructured devices was not possible until the 1990s, with the arrival of high precision industrial tools for microelectronics. The first article presenting MN for transdermal administration was published only in 1998 (4). MNs have been shown to enter the skin through the stratum corneum (SC) and the viable epidermis (VE), avoiding contact with nerve fibers and blood vessels that predominantly reside in the dermal layer. Therefore, the main benefit of using MN is the promise of a painless supply of low and high molecular weight active pharmaceutical ingredients. Skin has long been recognized as a potential target for local and systemic drug supply, as well as for vaccination. However, the practical value of the transdermal drug delivery route is limited by the substantial barrier properties of the skin. The physiologically beneficial protection provided by the skin against the penetration of xenobiotics is a disadvantage from the point of view of percutaneous transport of therapeutic agents. Therefore, a delivery system that temporarily and reversibly permeabilizes the skin can allow the delivery of a broad spectrum of molecules through the skin. One of these technologies is the microneedle, a micrometric needle that can create microscopic pores in the stratum corneum and upper layers of the epidermis, improving the permeability of skin by several orders of magnitude. The following review focuses on the various types of microneedles and their viable applications and certain trial reports.

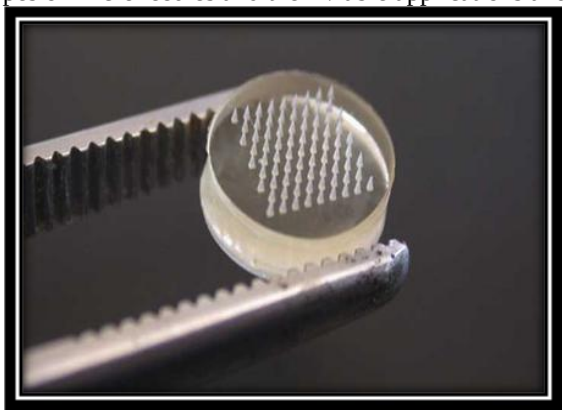

Figure 1 MICRONEEDLES

II. TRADITIONAL TYPES OF MN AND FABRICATION METHODS

2.1Methods of MN preparation

2.1.1 Traditional methods for preparation of MN

The first solid MNs were made from silicon using micro-fabrication technology to facilitate the passage of the chemical molecule, calcein, through the skin. In an experiment conducted by Sébastien, an attack using reactive ions was used to obtain a MN of a length of about 100 microns. This method of etching with reactive ions was a dry etching technology. With the exception of dry etching, there was another method of making MN, called wet etching. The main difference between these two approaches is that wet etching uses 30% potassium hydroxide (KOH) as the etching agent in place of sulfur hexafluoride (SF6) / oxygen (O2). The wet etching process is similar to dry etching. The key to the treatment step is the concentration of KOH and the ambient temperature (5). The two methods are:

Wet etching: In this process, the material is removed by dipping the wafer into a liquid bath containing a chemical etchant. The two main wet etching techniques are isotropic etching and anisotropic etching. Isotropic strippers attack the material, such as oxide, nitride, aluminum, polysilicon, gold and silicon, at the same speed and in all directions. They remove the material horizontally under the etching mask. On the other hand, the anisotropic etching agents attack the material (silicon wafer) at different speeds in different directions, to produce more controlled forms. Crystalline planes in silicon limit wet anisotropic etching (6).

Dry etching: This form of etching is performed at low pressure in the presence of inert or reactive gases. Dry etching is divided into two main types: reactive ion etching (RIE), which involves chemical processes, and ion beam milling, which involves purely physical processes.

The manufacture of lithography, both in microelectronics and in micro-machining, begins with lithography (lithos "stone" and "written" gráphein); the technique used to transfer the main pattern onto the surface of a substrate (for example a silicon wafer), previously coated with a photosensitive material, by selective exposure to a source of radiation (for example ultraviolet light). The most widely used type of lithography is photolithography. In recent years, more and more materials have been used to prepare MN, such as metal, polymers and ceramics. LIGA is a new approach to MN preparation. The LIGA process is a German acronym for Lithography, Galvanoformung, Abformung (Lithography, Electroplating and Molding). It is a kind of micro-machined technology based on X-ray lithography. This technique consisted mainly of three stages. They are, respectively, deep synchrotron X-ray lithography, electroforming microstructures and the reproduction of injection molds (7).Novel MN arrays fabricated by combination of other techniques

In recent years, many new MNs prepared with the combination of other devices have emerged. A new way to combine MN and sonophoresis has emerged. A Han study focused on the mechanical theory of the combination of ultrasound and ND. It has been shown that, compared to MN or ultrasound alone, the amount of BSA release increases doubly by using hollow MNs with ultrasound. This review has demonstrated potential for the combination of MN and ultrasound as a novel form of transdermal drug delivery. In addition, there was a new combination of three technologies. They were MN, electroporation (EP) and sonophoresis (SN). The combined use was to improve the penetration of the hydrophilic macromolecule skin. Drug penetration using 3 combined methods was shown to be 1.8-fold and 3.2-fold greater than MN + EP, MN + SN, and the drug penetration amount of 3 combined techniques was almost 80 times greater than MN, EP, SN only. To administer high molecular weight therapeutic agents, biodegradable chitosan-graphene nanocomposites of magnetic quantum dots were formed in MN matrices, where the water-soluble biocompatible polymer (PEG) was melted at the base of MN as part of detachment (8). Rapid separation MN, composed of PVA (separable arrowhead) and a poly (L-lactide-co-D, L-lactide) (PLA) support matrix, were prepared to fit into the skin itself in a very humid atmosphere due to sufficient mechanical force In an attempt to minimize the foreign body's response to invasive intracortical electrodes, a water-soluble and water-soluble sucrose-based MN ratio was developed. . It allows the direct surgical implantation of soft and flexible microelectrodes. To date, there are more and more silicon MN sensors, such as a micro / nano electrochemical sensor with hierarchical surface. This sensor was manufactured by combining MN and a multistage carbon nanotube forest (MWCNT), which can increase the electroactive surface. This MN sensor had three electrodes, and they respectively worked with an iron-based catalyst electrode, an Ag / Agcl electrode and platinum nanoparticles. The sensor was shown to react when the glucose concentration ranged from 3 to 20 m / M in a 0.01 M PBS solution. In vitro experiments showed that this sensor had a better sensitivity of 17.73 ± 3. μA / mM. cm2 relative to the matrix of nanotubes Au, Pt nanoporous and Pt MWCNT. Today, Strambini manufactured a new standalone MN with a built-in glucose biosensor on the back of the needle vessel. In the manufacturing process, the screen printed graphite electrodes were modified with the enzyme glucose oxidase and the MN chip was trapezoidal (9).Types of microneedles

2.1.2 Silicon MN

Silicon MN Silicon MN arrays have been widely used for decades due to good strength, easy fabrication methods. The first MN was fabricated by using standard micro fabrication techniques to etch arrays of micron-size needles into silicon. This MN, whose height was 450-500 μm and aspect ratio was around 4.5:1 was fabricated by dry etching technology. The final angle was 84. Nevertheless, a wet etched MN array with an angle of 45 was 280 ± 5 μm high with an aspect ratio of 3:1. It was observed that the former MN had the highest needle density, while MN fabricated by wet etching always had good surface properties. Melissa et al. did in vitro and in vivo experiments to investigate the characterization of micro electromechanical MN through skin . In vitro experiments showed the solid silicon MN increased 10-fold transdermal flux of calcein and increase in diameters of MN was approximately proportional to increase in flux. However, blood glucose concentration was not decreased significantly after hollow MN insertion by in vivo experiments(10). Furthermore, Haq et al. conducted clinical tests on skin response after wet-etched silicon MN treatment. In this study, twelve subjects accepted the treatment of hypodermic needle and MN with a height of 180μm, and 280μm, separately. Then researchers analyzed skin puncture, pain and sensation. It showed that wet-etched MN caused less pain and sensation compared to hypodermic needle with micro-conduits for delivery drug. Recently, Conor O'Mahony and his coworkers analyzed failure mechanisms of wet-etched silicon MN as well as reliability via in vivo experiments. This study demonstrated that many factors caused failure of preparing MN, like compressive forces or shearing force or other things. More mechanical tests need to be done to offer an optimal model for fabricating MN with good structure properties. Today, mesoporous silica nanoparticles loaded with diphtheria toxoid can be coated into hollow MN which was prepared by etching of fused silica capillaries with hydrofluoric acid. Resnik also performed experiments to evaluate skin penetration efficacy by Au-coated Si MN. Here, Au was used as an electrode for revealing electrical skin impedance change under MN force. Chicken skin, porcine skin and human skin were investigated in vitro and in vivo studies. Mechanical characteristics were also studied by equivalent applicators to accomplish an efficient skin penetration (v=3.6 m/s, MN array of 100, delivering 160mJ energy) Silicon and silicon dioxide materials are common materials for manufacturing micro-needles. They present good sensing and electromechanical properties, and their micro-processing technology for mass production is mature. However, the silicon MN arrays are easy to fracture in the skin during penetration(11).

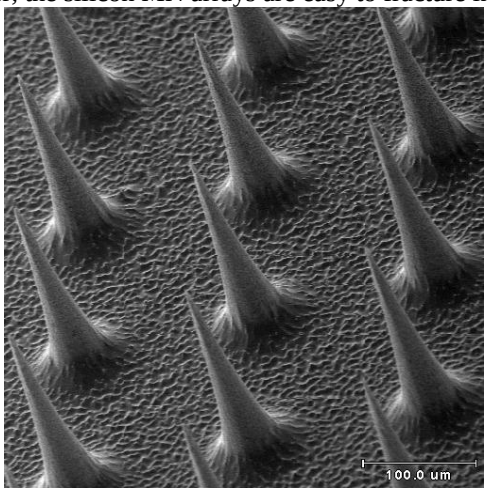

Figure 2 Silicon MN

2.1.3 Metal MN

The first micro-machined needle assemblies coupled to a metal fluid were manufactured by micromachining for fluid extraction and the metal sidewalls were finally deposited. Then, Martanto fabricated a solid metal matrix MN using an infrared laser to cut stainless steel sheet needle structures. The MN (50 μm × 200 μm) contains 105 needles with an angle of 20. In addition, the matrix of hollow micro-machined metal needles has an advantage over the other MNs in terms of protein intake and other biomedical applications. An MN-optofluidic biosensor composed of a micro-machined hollow metal needle integrated with microfluidic and photonic components can be used for the therapeutic monitoring of drugs in biological fluids. The hollow metal MN has been designed for reliable intradermal injection. As part of this investigation, Norman investigated a high-performance micromoulding process to produce MN metal with complex geometries. The main structure was a model for several replicas of poly (lactic acid-co-glycolic) micromolded (PLGA) and the structure was deposited on gold. Then, the polymer replicon was dissolved to produce a hollow metal MN after electrodeposition with nickel selectively outside the cavity. In such a

case, the hollow metal MN was strong enough to allow reliable insertion into the skin. Recently, Zhu made the Ni MN cone out of the plane using micro-molding and electroplating technology. This MN had a height of 300 μm and a density of 10-30 mA / cm². MN metal can also be used for intradermal immunization which has been coated with polyphosphene polyelectrolyte as a micro-manufacturing material and an immunoadjuvant compound. In this study, MN matrices were produced in two stages. First, the metal rods were made by etching a titanium foil with hydrofluoric acid and then bent out of the 90 ° plane. Following, MN was coated with a PCPP protein formulation during the micro dip coating process. It has been shown that protein release can be modulated from this coated MN. MN metal matrices cost less than MN silicon, while hollow metal MNs could be blocked during skin insertion. This problem must be solved urgently (12).

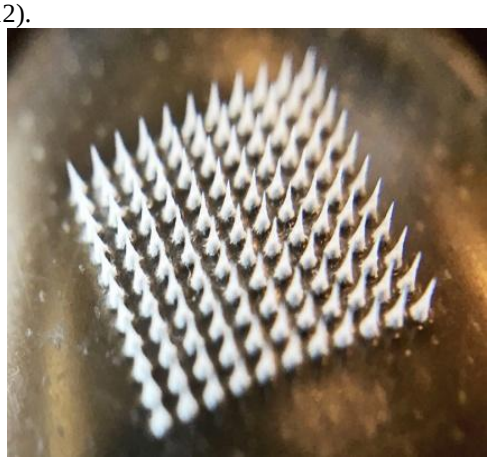

Figure 3 Metal MN

2.1.4 Polymeric MN

The MN polymer has attracted attention in recent years. Jung-Hwan et al. introduces three manufacturing methods for the economical mass production of biodegradable polymer MN. Like the fabrication of the MN metal, the beveled MN was fabricated with SU-8 epoxy by ultraviolet (UV) lithography. During the manufacture of the chisel tip, MN used a combination of wet silicon etching and reactive ion etching. Jung-Hwan has proposed a new lens-based lithographic approach to make conical MNs, which could control the geometric properties of the MN. It has been shown that these polymeric MNs are powerful enough to penetrate the skin without breaking down. MN containing poly-lactide-co-glycolide has also been shown to exhibit high mechanical strength, which has a potential for controlled release of the drug. Polylactic acid (referred to herein as PLA) is the most widely used polymeric material. Aoyagi et al. MN is manufactured with a high form factor of 100 (diameter: 10 μm, depth: 1 mm) of biodegradable polymeric material (PLA) n using a UV excimer laser. Later, a biodegradable polymer needle with several corner angles appeared. The fabrication of PLA MN with peak angles has been studied by simulating the finite element method (FEM). The electromagnetic force means that the angles of the tip become sharp when the needle becomes thin. This theory has also been applied to the study of the insertion mechanism of the mosquito probe. After that, Han proposed a new manufacturing method for preparing MN matrices embedded in grooves using PLA. The manufacturing process of this MN consisted of three steps. This was a standard 3D ultraviolet lithographic manufacturing of 3D cutting vessels, nickel electroplating production grooves, embedded shafts and a hot foil stamping process, respectively. 3D MN was manufactured using this method (880 ± 20 μm high, 710 ± 15 μm wide, 145 ± 15 μm thick) (13). Intradermal immunization experiments focused on the loading capacity of drugs of three types (A, B, C) MN. The specific surface area of the three MNs was 393, 418, 448 (103 nm3) respectively. Their drug loading capacities were 393, 1125, 2776 (103 nm3), respectively. It has been shown that the larger the area of MN, the greater the drug carrying capacity. Therefore, the MN incorporated into the slits could be an improved method for intradermal vaccination. A microneedle patch based on polycarbonate was also manufactured. In recent years, the biopolymer MN has appeared in several morphologies, such as droplets, porous polymers having various characteristics of strength and fluid transport. To administer liquid drugs, the acrylic channel is manufactured using 3D printing. To date, new manufacturing methods have attracted the attention of researchers. The Spatially Discrete Thermal Spinning (SDTD) method has been developed to produce tapered biodegradable MN. The photomask was made from a microinjection matrix consisting of convex and convex microlenses for the manufacture of polymeric MN. The MN solution was made using photomascaras, which could accurately control the drawing time and viscosity of maltose. The limitation of the traditional method of microcastering has been overcome. A biologically compatible MN matrix was prepared with sumatriptan succinate 10% w / w, PVP 30% w /

w, 1% glycerin, 1% polysorbate 80 and 58% water. In vitro studies showed that the drug flux obtained from this MN was 395 ± 31 µg / cm2 h over a 7-hour period with a delay time of approximately 39 min, which was a significant increase over transdermal patch. Traditional. MN polymeric polymers made from biocompatible materials can be safe for human health, and the process of preparation is simple and free. (14)

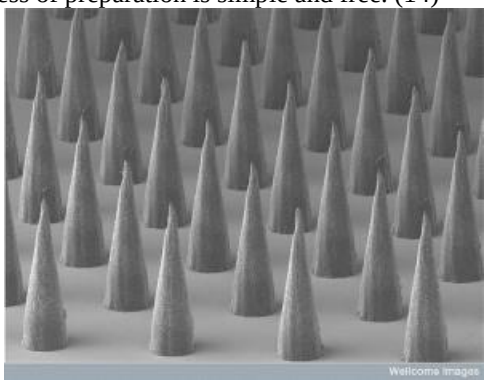

Figure 4 Polymeric MN

2.1.5 Ceramic MN

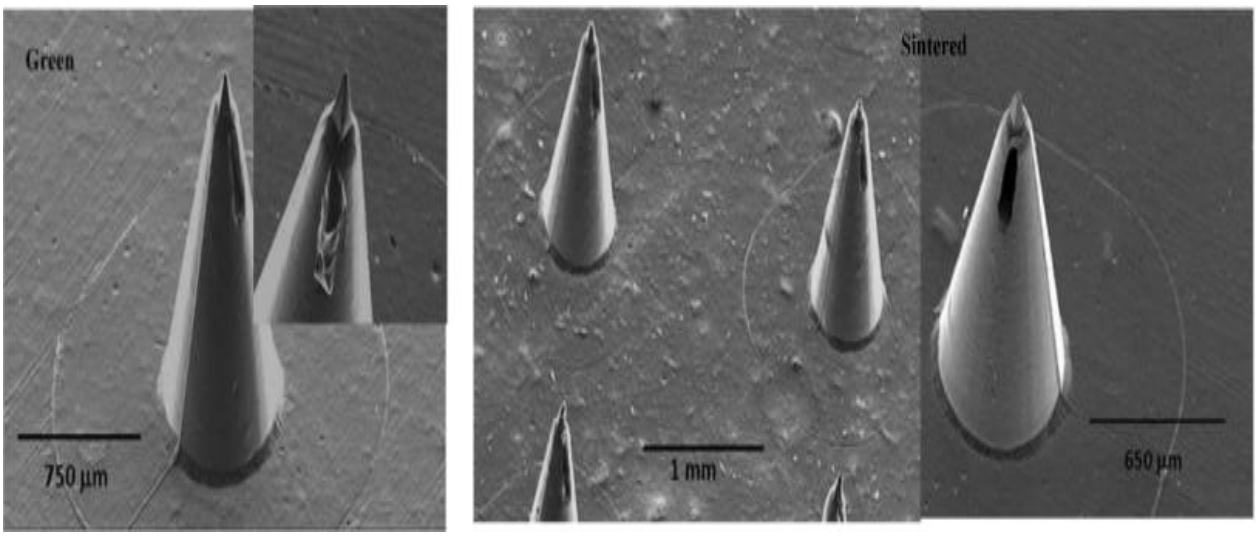

Figure 5 Ceramic MN

MN The process of manufacturing ceramic matrices MN (MNA) has appeared over the past decade. The process involved manufacturing a SU-8 / Si master and dual replication. In addition, the multiple replication of the PDMS mold offered an inexpensive production mold that could be reused for micromoulding in ceramics. Michel recently studied MN nanoporous ceramic matrices as a transport interface. In this study, the slurry was introduced into PDMS molds for ceramic melting and ceramic samples were examined to determine the porosity measurements. Until now, MN bioceramics have been developed with a flexible and self-igniting substrate. This design used the swelling and dissolving substrate to separate the substrate from the needles after insertion. Simultaneously, Cai et al. explored the design of two types of bioceramics MN (BCMN). One was BCMN G450 (height 450 µm, width 285 µm, distance from two dives 820 µm, tip radius 5 µm), the other was BCMN G600 (height 600 µm, width 380 µm, distance from two dives 91 6 µm, tip radius 5 µm). In the drug release study, the amount of drug released by BCMN in 4 hours was almost 4 times higher than that of SCMN (bioceramic MN matrices preloaded with a rigid substrate). The depth was 100 µm and 200 µm, respectively, after the penetration of G450 and G600 MN into the skin. This work has shown that MN bioceramic is an improved tool for transdermal drug delivery (15).

2.2 Consideration of MN design and skin properties

Regardless of the manufacturing methods described above, NDs must be able to demonstrate sufficient resistance to penetrate the skin or other biological tissue without breaking or bending before or during insertion (16). The main factors responsible for the performance of the MN are the type of material, the height of the needle, the radius of the

tip, the diameter of the base, the geometry of the needle, the thickness of the needle and the density of the needle. which, in turn, determine the general insertion and breaking strength of the MN. Understanding these relationships will enable the design of "smart" or "optimized" MN, with low insertion force and high fracture force. In doing so, it is necessary to understand the essential technical properties of the skin, in particular SC and viable epidermis (VE). Kendall has studied the mechanical properties of skin by penetrating intact SCs and VEs to efficiently direct molecules to immunologically sensitive cells in viable skin using micronanoprojections in a patch. The study determined the storage modulus, Young's modulus, and skin breakdown resistance, through SC and VE layers, in intact murine mouse skin recently removed using a microindentation probe installed in a NANO-indenter. It was observed that the mechanical properties mentioned above decreased with depth across the SC. The authors indicated that variation in skin properties, such as variation in thickness in different sites of the body, and variation related to age, sex, race, and body mass index (IMC) required special attention to ensure: consistent performance of the MN. Laurent studied the effect of age, race, BMI, sex and skin thickness variation in the body in 342 adult subjects (205 women, 137 men, 101 Caucasians, 118 Asians and 123 African blacks) and evaluated the efficacy of the intradermal injection by 1.5 mm long 30G MN. The results showed that the average thickness of the skin (epidermis-dermis) was 2.02 mm in the deltoid, 2.54 mm in the suprascapular, 1.91 mm at the waist and 1.55 mm in the regions. of the thigh. Regardless of age, race, BMI, or sex, MNs 1.5 mm long could be used effectively for i.d. SC thickness variation with body location, sex, age, and skin condition has also been reported. Davis first studied the influence of MN geometry on the insertion force and the fracture / buckling force. MN (0.1-3 N) insertion forces varied linearly with the interfacial area of the needle tip and the fracture force increased with increasing thickness, angle and radius of the wall. . . However, the safety margins (ie the relationship) between the fracture force and the insertion force were high. Davidson quantified the influence of different geometric parameters, such as MN thickness, MN diameter, drug embedding depth on MN (ie, the distance of the tip covered by the drug film), the depth of penetration, the space between MN and the matrix pattern, associated with six different solid forms of drug coated MN. The objective of the study was to identify the most efficient MN geometry for effective skin permeation. The study was conducted in a 3D model using FEMLAB scientific modeling software. It has been found that penetration depth and spacing between centers and MN centers significantly affect effective skin permeability (Peff). On the other hand, the other dimensions of MN, such as the diameter of the cylindrical MNs, the thickness of the flat MNs and the depths of the coating, were less significant for Peff. In general, the largest, longest, and most heavily loaded MNs gave a larger Peff. The effective insertion of the MN with a minimum of pain can be achieved through the use of a vibrating MN device, controlled by a mechanical actuator, similar to that of the vibratory cutoff action (frequency 200-400 Hz) of the mosquito. Yang and Zahn studied the effect of vibratory performance on MN insertion force. The results showed a significant decrease (greater than 70%) of the insertion force thanks to the use of a vibratory drive. This was due to three simultaneous factors, namely increased stiffness of the skin, tissue damage due to cavitation due to vibratory waves and localized thermal damage due to frictional interactions between the MN and the skin. (17)

2.3 In vitro and in vivo drug delivery mediated by MNs

Solid MN Assisted Drug Distribution Solid MNs can be used to mechanically interrupt SC and create transient pores of micron dimensions. When administering SMN-based drugs, SMNs are first pressed against the surface of the skin, followed by the application of traditional patches containing drug molecules. Molecules with powerful physicochemical properties have been delivered through the use of SMN. Martanto (18) used MN matrices (7 × 15) for transdermal insulin delivery in models of diabetic rats. During and after the treatment with MN, an insulin solution (100 or 500 U / ml) was brought into contact with the skin for 4 hours. NDs were withdrawn at different times and it was observed that blood glucose levels had decreased by 80%, a similar effect to 1.6 to 4.1 mU (0.06 to 0.15 μg) of insulin injected subcutaneous. Chang (19) developed an integrated MN roller (230 μm), creating 267 holes per cm2 per treatment. After treatment with an MN roller, the penetration rate of the ovalbumin, insulin and fluorescein-labeled bufexame isothiocyanate (FITC) increased significantly, respectively from 13.4 to 83.3, 10.1 to 110.6 and 11.9 to 242.6 pmol / cm 2. Pearton evaluated gene delivery using a trunk-shaped MN silicon matrix (with a 4 × 4 matrix, a height of 260 μm and a base width of 200 μm). It was confirmed that the application of micropores MN created depths of 150 to 200 μm deep in the skin and increased transepidermal water loss. It has been demonstrated that the subsequent application of Carbopol®-940 (1% w / v) and a thermosensitive triblock copolymer of PLGA-PEG-PLGA hydrogels (23% w / w), containing a known concentration of Plasmid DNA (pDNA) in NM-created microconductors capable of releasing pDNA in its functional form for gene expression in viable tissue. In an in vitro study, Badran (2009) pre-treated abdominal skin samples in humans with Dermarollers®, composed of different heights of MN. Invasomes (100 nm diameter) containing hydrophilic model drugs (radiolabelled mannitol and carboxyfluoroescein) were applied to pretreated skin samples. Model drug penetration

was greater across skin samples treated with Dermaroller®. This was further increased by invasomes compared to aqueous solutions of model drugs. Invaders resulted in greater penetration due to their flexibility and improved penetration properties. In 2009, Ding investigated NM-mediated immune responses in a mouse model after transcutaneous immunization using Diphtheria Toxoid (DT) model antigen. DT, when applied to intact skin, produces low levels of IgG. However, the skin pretreated with MN had significantly higher IgG titers, which increased further in the presence of cholera toxin. Pastorin recently used vertically aligned vertically aligned pyramidal nanorods (nanoneedles). Their length was less than 50 μm and their base diameter at 150 nm. The distance between the adjacent bars was 300 nm. It has been reported that these nanoneedles were sufficient for the administration of the vaccine and, more importantly, the nanopores created were closed immediately after removal of the nanoneedle. In addition, we have previously demonstrated the use of solid silicon MN matrices to improve the skin penetration of 5-aminolevulinic acid (ALA) in vitro and in vivo. Puncture of the murine skin removed with 6 x 7 MN templates (270 μm in height, 240 μm in diameter, and 750 μm spacing) resulted in a significant increase (from 178.82 nmol / cm2 hr to 427.80 nmol / cm 2 h), after 5 h, during the transdermal administration of ALA released from a bioadhesive patch containing 19 mg of ALA (cm - 2) (20).

2.4 Drug delivery and/or biological fluid sampling mediated by hollow MNs

HMNs consisting of a fine orifice can be integrated into a drug solution unit for continuous drug delivery or for sampling biological fluids, unlike the replacement of SMN with patches loaded with traditional drugs for administration of drugs. . Martanto quantified the relationship between perfusion rate and other parameters, such as insertion depth (900 and 720 μm), retraction distance (180 μm every 5 minutes) (ie MN is inserted into the skin at depth and then retracted to the desired height), perfusion pressure (69 and 172 kPa), needle type (beveled or blunt tip), tip opening size (22-48 μm) and presence of hyaluronidase (200 U / ml) The study used a single hollow glass MN, attached to a glass syringe of 250 μl or 1 ml (containing a solution of sulfurodamine B 1 × 10-3 M) and inserted into the skin of a human body. The infusion rate was measured in relation to the various parameters mentioned above. Insertion / retraction has been shown to lead to a significant increase in throughput. The increase in pressure was proportional to the increase in flow. The infusion rate of a MN with a beveled tip was three times that of a round-ended MN. The addition of hyaluronidase increased the infusion rate by a factor of seven. Infusion over time resulted in higher initial flow rates that quickly returned to steady state within minutes. Unlike other perfusion studies performed in hollow MN, this study shows strategies for increasing throughput using a well-designed perfusion and geometry protocol. In another study, Martanto showed that tissue compaction during infusion can be avoided by partial retraction, as well as by other approaches, such as the application of MN by the drill / vibration motion, and a longer insertion. fast. MN retraction resulted in tissue relaxation, which relieved skin compaction and increased local flow conductivity. Wang inserted the same MN hollow glass into the skin of in vivo hairless rats and human cadaver skin in vitro using rotary or vibratory penetration devices that pierced the individual MN or MN dies in the skin of the body. known depths. Compounds such as fluorescent calcein, insulin (100 U / ml, Humulin®), FITC insulin, polymeric microparticles or Caco-2 intestinal epithelial cells were administered using hollow MN and the images were taken by light field microscopy or optical microscopy. fluorescence Histological staining was performed to plot the depth of penetration. The results showed that rotating MN perforation in the skin can deliver the molecules at a precise depth with low penetration forces. Microinjection of MN at a depth of 800 μm and retraction at about 200 μm showed a greater accumulation of fluorescent calcein compared to insertion of MN without retraction. In addition, microinjection of insulin by MN, inserted at a depth of 500 to 800 μm and perfused for 30 minutes, resulted in a 25% drop in blood glucose levels below pre-treatment levels. When MNs were retracted by approximately 200 μm, blood glucose levels were reduced by 75% compared to pre-treatment values. The experiments also demonstrated the efficacy of microinjection of Caco-2 cells via MN at speeds up to 100 μl / sec without loss of cell viability. Higher pressures (2.5 to 20 psi) were required for delivery of microparticles to the skin. It has also been suggested that the vibration of the MN dies could also produce efficient microinjections similar to the rotating device. Therefore, this study demonstrated that the appropriate MN design and insertion protocol can be used to deliver macromolecules, microparticles and cells precisely to the controlled depth in the skin. Jiang used the HMN anterior crystal to overcome the ocular barrier, the sclera, for ocular drug delivery. Using the prototype HMN device associated with the previous syringe, the model drug sulforhodamine B, the nanoparticles (encapsulated with Nile red) and the microparticles (labeled with flurosein) were infused in volumes of 10 at 35 μl in the sclera tissue using individual MN, where the thickness of the sclera and the perfusion pressure have negligible effects on the fluid intake. Therefore, this study has demonstrated that HMN-assisted sclerotic perforation can facilitate the spread of the drug across the sclera into choroidal and retinal tissues to treat fundus diseases. Patel recently used the same 500 to 1000 μm long MN to deliver fluids and suspensions of polystyrene nanoparticles modified with carboxylates (20, 100, 500 and 1000 nm diameter) (up to 30 μL) in the supracorodial space of the

rabbit, Verbaan studied the in vitro transport of three different molecules of increasing molecular mass (blue cascade, Mw = 538 Da, blue cascade dextran, Mw = 10 kDa and FITC dextran, Mw = 72 kDa). through dermatomized human skin. The skin was previously treated with 4 × 4 assemblies of 30 G needles with a length of 300, 550, 700 and 900 microns. A significant increase in permeation of each of the three compounds was observed for pretreated skin samples compared to control skin. However, in these studies, MN matrices of 300 μm in length could not pierce the skin. The natural elasticity of the skin resulted in a skin fold around the MN of 300 μm. Subsequently, to overcome the elasticity of the skin, Verbaan investigated the effect of improved perforation using a variable speed electric applicator (1 and 3 m / s) and compared it to a manual applicator. Verbaan also studied triangular hollow silicon NM ~ 245 μm in length and 250 μm in base, with densities of 4 × 4, 6 × 6 and 9 × 9. At a speed of 3 m / s, electric applicator It has proven superior to a manual applicator to create skin-like channels on a reproducible surface, for MNs of 245 and 300 μm in length. Regardless of the density of the matrix and the type of MN, the use of the electrically operated applicator resulted in a significant increase in the cascade of blue flow through MN treated skin compared to the manual applicator. For example, the flow of blue cascading through the manually perforated skin using the 4 × 4 assembled hollow metal matrix was 9 ± 4 pmol / cm 2 / h, while the flow was 55 ± 11. pmol / cm2 / h when operating at a speed of 3 m / s with the electric applicator. In another study, Nordquist designed a patch-like integrated MN device (Figure 2c), which was used to administer insulin to 61 diabetic rats divided into seven groups. For example, the average plasma insulin concentration after 210 minutes of infusion for intravenous (iv) administration (0.14 IU / h, 70 IU / ml) was 196 ± 20 μU / ml and for insulin infusion . High-speed MN-assisted intradermal injection (0.40 IU / h, 100 IU / ml) was 167 ± 15 μIU / ml, respectively. It has been suggested that this new concept of intradermal insulin delivery through these integrated MN devices, which not only control the release, but are also easy to use, and can replace the routine treatment with insulin under -cutaneous (sc) or iv (21)

2.5 Drug delivery mediated by coated MNs

It has been found that MN coating is an attractive technique for the rapid delivery of bolus molecules into biological tissues, particularly for the delivery of vaccines to the skin. In addition, the coating and drying of drug molecules on the surface of MN can enhance their long-term stability (22). Various techniques have been demonstrated to cover MN with molecules of different molecular weights. The two most commonly used coating methods for nanomaterials are immersion and casting techniques. Cormier demonstrated the immersion coating of a titanium matrix MN (Macroflux®) by partial immersion in aqueous solutions at 24 or 40% desmopressin and 0.2% polysorbate 20. In short, after coating with different amounts of desmopressin in the MN matrix (321 MNs / cm2, surface of 2 cm2, height 200 μm, width of the base 170 μm and thickness 35 μm), the matrix was fixed to an adhesive patch (patch surface 5.3 cm2) and applied using a prototype patch applicator. The patch-coated MN matrix delivered 20 μg of desmopressin in 15 minutes in a hairless guinea pig model and the bioavailability was 85%. Widera, from the same research group, presented titanium MN matrices with immersion coating (width 100 μm and thickness 35 μm) with the model ovalbumin antigen (OVA). The number of coatings and the OVA concentration in the coating formulation were used to control the amount of OVA coating relative to the MN. Patches of different tip shapes and densities of MN were applied in vivo to the hairless guinea pig skin (HGP). The influence of the depth of administration of the vaccine, the dose of vaccine administered, the density of MN and the field of application was studied. The presence of anti-OVA (IgG) antibodies in the immunized HGP sera was evaluated, which was determined by an enzyme-linked immunosorbent assay (ELISA). It has been observed that the immune response was dose dependent. Gill and Prausnitz have designed new MNs with central openings called "pouches" (Figure 4a), which have been dip-coated with model drugs and various surfactants and viscosity improvers, prepared in aqueous or organic solvents. . It was concluded that coating solutions with lower surface tension facilitated good wetting and reduced the rate of film formation on the MN surface. On the other hand, a higher viscosity resulted in a higher volume of liquid film adhesion and residence time at the MN surface. The versatility of this coating technique has been demonstrated by coating the hydrophobic molecule, curcumin and model proteins, BSA and insulin, in organic or aqueous coating solutions. In addition, up to 1 mg of a model drug, riboflavin, was coated in MN matrices of 10-20 cm 2. A composite filling of the pockets in the MN has also been demonstrated, where multiple coating with more than one drug formulation with intermittent wash cycles has been achieved. Gill and Prausnitz in 2008 also demonstrated the isolation of drugs in MN pockets and the overlap with another protective layer (eg, PLGA) followed by a second drug layer. The bags could also be filled with liquid drug formulations, held in place by the surface tension. Using similar stainless steel MNs, Jiang proposed administering drugs to the eye using 500-700 μm long MN coated with fluorescein and pilocarpine. The fluorescein coating dissolved in less than 30 seconds in a human cadaverous scleral model in vitro. The bioavailability of fluorescein and pilocarpine, when administered by MN, was 60 and 45 times higher than that achieved by topical application, respectively, in an in vivo rabbit eye

study. The MNs embedded in the grooves (type A, type B and C), shown in FIG. 5, were dip-coated with three different loads of ovalbumin (1, 10 and 100 μg / ml) and tested for immunization. in the mouse. skin. The degree of immune response was higher in type C MN, followed by types B and A. This result suggests a higher load capacity of antigens in grooved MNs (types B and C) compared to smooth (type AT); therefore, MNs incorporating grooves exhibited a maximal immune response. In 2009, in a recent study, Kim investigated the stability, immunogenicity, and protective immunity of immunodeficiency markers made of inactivated influenza virus-infected NMS. The NMS were dip-coated six times in coating solutions containing 15% w / v trehalose and manually inserted into the skin of anesthetized mice. It was observed that the total antibody response (IgG) was significantly higher in trehalose-coated NMs than trehalose-free, which was similar to immune vaccination. Using a casting method, Xie et al. (2005) coated with MN (50-200 μm) model compounds (calcein and bovine serum albumin, BSA) dispersed in chitosan. A chitosan solution containing these model drugs was poured onto the MN chip and allowed to dry overnight at room temperature to form films. The influence of factors such as matrix thickness, drug content and matrix concentration was studied. The in vitro permeation rates of calcein were 50 and 1 μg / cm 2 / h, respectively, with and without MN (23). Permeation of BSA increased with decreasing chitosan content and increasing BSA loading; while the rate of permeation decreased with increasing film thickness. MN enhanced TDD can also be achieved by pressing the MN against a skin surface previously coated with drug solutions. Jae-Ho used polycarbonate MN matrices and studied the permeation of calcein on excised rat skin in a Franz cell apparatus. An amount of 0.1 g of calcein gel directly coupled to the polycarbonate MNs (height 500 μm and 154 cm-2) showed a permeation of 5.46 times greater than the permeation after 12 hours of penetration into the skin of the excised rat. compared to the calcein gel alone. In addition, an increase in the MN matrix density of 45 to 154ea / cm 2 increased the calcein flux from 30.14 to 54.13 ng cm -2 h -1 from the calcein gel. Drug delivery mediated by dissolving MNs

Compared to other MN application techniques, the main advantage of these MN types is the dissolution or biodegradation of the MN material. This type of delivery system depends essentially on the dissolution of the MNs when they come into contact with the interstitial fluid of the skin. This process (depending on the material of MN) releases the drug molecules from the matrix for local or systemic delivery. So far, most soluble NMs have been made using simple sugars and polymers using mainly molding or molding techniques. Miyano was the first to report the production of manganese from natural sugars. The maltose powder was heated at 140 ° C for 1 hour to form sweet maltose. The powdered medicine was added to this candy and mixed evenly in one minute and stored in a dry environment at room temperature. Small amounts of this maltose-containing drug were placed in an MN foundry mold at 95 ° C and molded into MN dies. Using this method, matrices of 500 μm high MN containing ascorbate-2-glycoside (5% w / w), sodium salicylate (10% w / w) and calcein (10% w / w) p) have been manufactured. MNs dissolved within a few hours at a relative humidity of more than 50%, but retained their shape for at least 3 months with 40% humidity. He prepared MN from a wire-forming biopolymer (dextrin), and the MNs obtained were evaluated to determine their percutaneous insulin supply. After administration of these self-dissolving mouse-loaded MNs to mice, dose-dependent hypoglycemic effects were observed and insulin was found to be stable in MN for one month at 40 ° C. Polypropylene was immersed in the dextrin gel and stretched perpendicularly to form wire-shaped needles, which were dried at 4 ° C in a desiccator. Similarly, erythropoietin (EPO) loaded polymeric MNs prepared using a yarn-forming method for the percutaneous administration of EPO in mice were prepared. The wire-forming materials used in this study were dextrin, chondroitin sulfate, and albumin. Relative bioavailability was 82.1%, 59.7%, and 78.6% for NDs made with dextrin, chondroitin sulfate, and albumin, respectively. In another study, Ito et al. (2008) prepared NMs with automatic dissolution from dextrin, chondroitin sulfate or dextran containing low molecular weight heparin (LMWH) (Mw = 4.5 kDa), basal length and MN being 1.5 mm and 0.5 mm. respectively. At 100 IU / kg LMWH in in vivo rat studies, the bioavailability was 97.7, 81.5 and 102.3% for dextran, chondroitin and MN for dextrin. respectively. In addition, it was found that the content of LMWH loaded in dextranMN was stable for at least 3 months when stored under three different conditions, namely 40 ° C, 4 ° C and -80 ° C. Kolli and Banga used solid maltose MN by micro-molding techniques, for the immediate administration of nicardipine hydrochloride (NH) through the skin of rats. Tetrahedron MNs, with 500 μm heights and 150 μm intervening spaces, were used to treat rat skin in vitro and in vivo. In in vitro studies of Franz cell diffusion (where the donor compartment was composed of 500 μl of NH 10 mg / ml), MN-treated full-thickness rat skin showed an almost 4-fold increase in penetration. transdermal NH with respect to passive diffusion. In the in vivo studies, the plasma NH level (Cmax) was 56.45 ng / ml (after approximately 7 h) in MN-treated rats, but detectable levels for passive NH after 8 pm (with a Cmax <20 ng / ml). Similarly, Guohua 2008 investigated the effect of similar MNs on soluble maltose in the permeation of human immunoglobulin IgG (Mw = 150 kDa) in rat skin in vitro.

The influence of parameters, such as the length of MN (200 and 500 μm), the number of MN and the concentration of the drug in the in vitro administration throughout the rat skin, was evaluated. In general, the flow rate of human IgG increased from 27 to 102 ng / cm 2 h when the height of the needle was increased from 200 μm to 500 μm. The

increase in the number of MN also increased the flow and the increase in IgG concentration up to 20 mg / ml increased the flow, after which (for 40 mg / ml) no significant change in flow rate been observed. This has been attributed to the saturation of the boundary layer with respect to the donor solution. In contrast, Donnelly (24) manufactured API loaded galactose MN. Due to the high processing temperature (i.e. 160 ° C) of MN galactose, substantial losses of IPA occurred, namely 5-aminolevulinic acid (ALA) and bovine serum albumin (BSA) during treatment. In vitro drug delivery experiments using MN matrices loaded with ALA revealed that less than 0.05% of the total drug load was released through a model silicone membrane. Similarly, only small amounts of ALA (about 0.13%) and undetectable amounts of BSA were administered when the galactose matrices were combined with aqueous vehicles. In addition, the galactose MNs were unstable at the relative humidity of the environment (43% and 83% RH) and became adhesives. Finally, the authors suggested that carbohydrate-based MNs were not the solution to the problems posed by the use of MN in silicon and metal. This is especially true as MNs produced from hot melt polymers also suffer a substantial loss of drug during treatment. Park et al. (2006) manufactured MN beveled PLGA using a micro-molding technique to encapsulate model drugs (calcein and BSA). The drug molecules were incorporated directly into the PLGA (rapid release) needle matrix or as double encapsulation, first encapsulating the drug in carboxymethylcellulose (CMC) or poly-L-lactide microparticles. then encapsulating the drug-laden microparticles. on needles (for controlled / delayed release). The calcein diffusion rate of PLGA-MN was 1.2 × 10 -10 cm 2 / sec, that of MN loaded with CMC microparticles was 4.7 × 10 -12 cm 2 / sec and that of MN loaded with microparticles. PLA was further reduced. more at 6.2 × 10-10 cm2 / s. Kwon (2004) has proposed a transdermal patch for drug delivery, which consists of dissolving MN. A material generally considered safe (GRAS), sodium carboxymethylcellulose (SCMC), was loaded with lidocaine hydrochloride and melted in micromoldes, compressed and dried to form MN (550 to 650 μm long). In in vitro studies with human cadaver skin, the lidocaine hydrochloride flow rate was increased 4.8-fold relative to the rapidly dissolving MN matrix compared to the lidocaine solution (100 mg / ml). In addition, Kwon and Oh (2009) also demonstrated the use of parathyroid hormone (PTH) in in vitro and in vivo studies in the treatment of bone regeneration using SCMC soluble MNs. (height 1500 μm and μm wide) Miyano developed a hydrolytic MN of maltose and poly (ethylene glycol) (PEG, Mw = 600Da). The fast-dissolving maltose MNs were one-dimensional 500 μm long tetrahedral MN, which dissolved within 3 hours of insertion into the skin. However, high viscosity and poor performance prevented the manufacture of maltose MNs deployed in 2D matrices. On the other hand, the low viscosity of PEG not only allowed the production of high performance PEG MN, but also the fabrication of 2D PEG MN matrices with a length of 1000 or 2000 μm, respectively. In contrast to typical high temperature molding or methods unsuitable for mass production of polymer nanoparticles in solution, Sullivan proposed the photopolymerization (100 W UV lamp at a wavelength of 300 nm) of a liquid monomer, vinylpyrrolidone. . NDs prepared using this method were loaded with 0.2% BSA of Red Red BSA, which dissolved in the minute following pig's skin insertion. A 1 mg dose of β-galactosidase when encapsulated in MN maintained similar enzyme activity to a solution of β-galactosidase in PBS. Jeong proposed molecules encapsulated in pyramidal MNs, which dissolve in the skin by bolus or sustained release over time (168 h) when encapsulated molecules are observed in the MN support layer. MNs were made from carboxymethylcellulose (CMC), amylopectin (AP) and bovine serum albumin (BSA) using molding techniques. The model drugs, sulforhodamine B (0.15-30% w / w), BSA (20% w / w) and lysozyme (5% w / w) were encapsulated in MN or in the carrier layer or both for insertion studies. and release of the skin. . For example, Figure 6b shows the release of sulforhodamine B after dissolution of CMC MN (Figure 6a) over time. The mechanical properties of the MN (height 600 μm, base width 300 μm and separation 600 μm) were classified from highest to lowest as follows: AP, CMC / BSA (80/20% by weight), BSA and CMC II It is interesting to note that the encapsulated lysozyme was stable for 2 months at room temperature (25).

2.6 Drug delivery mediated by combination of MNs and other techniques

Various enhancement techniques associated with MN have also been investigated to further improve drug delivery through MN-induced micropores. The synergistic effect of MN and iontophoresis (ITP), nanoparticles, or both, has recently been studied. Wu et al. (2007) studied the combined effect of pretreatment with MN and ITP on the in vitro permeability of low molecular weight and high molecular weight D2O of FITC-dextrans, with average molecular weights of 4, 10, 39, 71 and 200 kDa, respectively. The results indicated that the passive permeability of D2O was almost similar to that of the combined effect of MN and ITP, while a significant increase in FITC-dextrans flow was observed when MN and ITP were used together. However, permeation decreased with the increase in FITC-dextrans MW. Vemulapalli investigated the synergistic effect of ITP and the soluble MNs of maltose (two rows of 28 MN each with a height of 500 μm) in the permeation of methotrexate (MTX). In in vivo studies in rats, it has been demonstrated that the combined effect of MN and ITP results in a 25-fold increase in MTX delivery relative to MN or ITP alone. Katikaneni used the same MNs for maltose (six rows of 27 needles each) in combination with PTI for

the supply of a high molecular weight protein, daniplestim (molecular weight of 12.76 kD). A significant increase in danestim permeability was observed from 0 to 718 ng / cm 2 (in TRIS buffer at pH 7.5) and from 555 to 22 728 ng / cm 2 (in acetate buffer at pH 4.0). Chen showed in vitro permeability of insulin nanovesicles, various potentials and zeta diameters. Penetration of insulin nanovesicles through guinea pig skin was significantly greater than that of insulin solution in PBS, which could not penetrate. Indeed, the soy lecithin contained in the nanovesicles has caused the disruption of lipid structures of the skin and, consequently, an improvement in the administration of insulin. However, nanovesicles could not administer clinically effective amounts of insulin. In contrast, the MN-mediated microchannels, in combination with ITP, showed effective insulin penetration. Insulin penetration rates of nanothexes induced by ITP through the skin with MN-mediated microchannels were 713.3 times higher than their passive diffusion. In addition, in vivo studies in the diabetic rat showed an effect similar to that of CS injections in the control of blood glucose. Qiu et al. (2008) studied a combined pretreatment method with MN and elastic liposomes to increase the penetration of docetaxel into the skin (DTX, Mw = 807.9) in in vitro models. DTX liposomal systems with and without elastic properties were prepared and characterized. Elastic liposomes dramatically improved the delivery of DTX to the skin compared to conventional liposomes and the control of 20% w / w saturated ethanolic solution without MN treatment. The penetration of elastic liposomes through the skin, previously treated with MN, reduced the delay time by nearly 70% compared to that obtained with conventional liposomes (26).

2.7 Human studies to demonstrate the clinical safety and efficacy of MN application

Although MN technology has been shown to enhance transmembrane delivery of a wide range of molecules, as demonstrated by in vitro and ex vivo models, only a few studies have reported the success of such devices in humans. . Kaushik conducted the first study in men, including 12 healthy volunteers, men and women, aged 18 to 40, to demonstrate that the application of MN was painless. The MNs used in this study had a length of 150 μm, a base diameter of 80 μm and a peak radius of 1 μm. Each set contained a total of 400 MN. The subjects' pain scores were recorded on a visual analogue scale (VAS) and it was found that the application of MN was painless and did not cause damage or irritation to the skin. Bal et al. (2008) investigated barrier safety and disruption after the application of MN matrices of different lengths and types in 18 healthy volunteers (nine men and nine women) aged 21 to 30 years. Parameters such as skin barrier function (measured by TEWL), erythema (assessed by skin staining methods and laser Doppler imaging (LDI)) and pain score were measured. The values of TEWL and erythema after treatment with solid MN matrices 400 μm in height increased significantly compared to 200 μm. However, for all MNs, the irritation was short-lived (<2 h) and the application was painless. Sivamani (27) studied the injection of methyl nicotinate into 11 healthy human subjects, using a pointed or symmetrical HMN matrix in silicon (200 μm long and 40 μm in diameter of light) and fixed at a syringe. It was observed that high MN injections resulted in higher blood flow than symmetrical MNs. Volunteers reported feelings of pressure but no pain when applying MN. The same workers also investigated whether MN silicon hollow matrices were able to penetrate and deliver drugs beyond SC in five human volunteers. Hexylnicotinate (HN), a lipophilic vasodilator, used as an SC penetration marker, was injected or applied locally to the forearm sites with adhesive tape, without tape. By measuring Doppler laser blood flow (LDI), MNs have been shown to be able to inject the drug beyond the SC. In addition, band extraction did not significantly benefit MN penetration, indicating that MNs avoid the SC barrier. Haq studied pain (using a VAS score of 0 to 10 cm) and sensory responses in 12 human subjects. Subjects received insertion of two different types of MN silicon (180 and 280 μm high and 6 × 6 series) and a 25G hypodermic needle. The average pain scores VAS were 0.25 and 0.60 cm for respective heights of 180 and 280 μm MN. EVA scores in subjects treated with a hypodermic needle were ≥ 1.25 cm. In addition, participants experienced greater "acute" and "throbbing" sensations with hypodermic needles, as well as more "pressing" and "heavy" sensations when applying MN. A methylene blue staining study showed that the micropores induced by MN close 8 to 24 h after the immediate withdrawal of MN. Wermeling conducted the first clinical studies in humans to demonstrate MN-based transdermal administration of a hydrophilic compound, naltrexone (NTX). The MNs used in this study were 620 μm high, 160 μm wide and 5 × 10 matrices (28). NTX adhesive patches were applied to the arm after treatment with MN and blood samples were taken for 72 hours. The results showed a rapid uptake (1.6 to 8.1 ng / ml) of NTX in the first hours following application, followed by a stable plasma concentration at about 2.5 ng / ml for 72 h. Damme (29) conducted a single-blind study to evaluate the safety and immunogenicity of intradermal administration of low dose influenza vaccines (α-RIX®) using a new MN device in 180 healthy men and women (aged 18 to 40). years). The MN (MicronJet ™) device consisted of a matrix of 4 MNs in silicon (450 μm in length) attached to the tip of a plastic adapter that could be mounted on any standard syringe. Subjects were randomized to receive a full intramuscular (IM) dose (15 μg haemagglutinin (HA) per strain) with a standard needle (IM group) or a low dose intradermal dose (ID1 group) (3 μg HA by strain) by MicronJet ™ or by mean intradermal dose (ID2 group) (6 μg

HA per strain) by MicronJet ™. It was concluded that low-dose influenza vaccines administered by MicronJet ™ produced similar immunogenicity responses to full-dose IM vaccines. Gupta et al. (2009) (30) tested the efficacy of hollow MN in insulin administration in adults with type 1 diabetes (male and female) versus that of a catheter infusion set (9 mm). MN was attached to a 3 ml syringe that was also connected to a syringe pump that controlled the rate of insulin delivery. The MNs were inserted at 90 ° into the abdominal skin at depths of 1-5 mm using a custom-made rotator. The results showed that the insertion depth of 1 mm MN in the skin resulted in rapid absorption of insulin and reduced glucose in fasted subjects. MNs inserted into the skin at 1 mm thickness were also found to be effective in reducing postprandial glucose levels. Subjects did not report any pain after MN application. Although few studies have examined the safety of MN application, the potential for microbial penetration into the viable epidermis by the microscopic pathways created by these NDs has not been reported. However, we have recently shown that microorganisms (Candida albicans, Pseudomonas aeruginosa and Staphylococcus epidermidis) can pass through MN-induced holes in the stratum corneum. However, the risk of infection associated with the application of MN on the skin is minimal and will likely be lower than that associated with hypodermic needles. Safety can be improved by sterile or aseptic manufacturing and the manufacture of MN from self-neutralizing materials (eg, solvent or biodegradable polymers) to avoid inappropriate or accidental reuse.

III. CONCLUSION

Promising MN drug delivery systems can be constructed with silicon, metal, polymers and ceramics, and can be used to deliver biopharmaceutical products such as insulin, vaccines, hormones, chemical molecules, proteins and peptides. The greatest benefit of this method of administration is to reduce pain and improve the effectiveness of drug delivery. However, there are some issues that need to be addressed in the field of ND research. The most important problem is the security of applications. The injection of MN is painless compared to that of a hypodermic needle. Different types of materials built with MN can also cause skin pain. In detail, factors such as the length, width, thickness, number and angles of the MN tip can influence the pain score of the human subject. Therefore, it is important to optimize the MN design and preparation process to reduce pain, for example by reducing the length and number of MNs. The depth and pressure associated with the injection must also be taken into account. In addition, the MN loaded with the current drug has low loading efficiency that can be affected by the forms. Therefore, the optimization of MN forms is considered as a potential method of improving the loading capacity of MN drugs. Although NDs are excellent drug delivery systems for transdermal delivery, many jobs are still needed before translating them into clinical use. In the future, further work will be devoted to the development of MN ceramics.

V. REFERENCES

[1] Kaushik, S., Allen, H.H., Donald, D.D., McAllister, D.V., Smitra, S., Allen, M.G., Prausnitz, M.R. (2001). Lack of pain associated with microfabricated microneedles. Anesth Analg. 92:502–4.
[2] Prausnitz, M.R. (2004). Microneedles for transdermal drug delivery. Adv Drug Deliv Rev. 56:581–7.
[3] Gerstel, M.S., Place, V.A. (1976). US patent US3964482.
[4] Henry, S., McAllister, D.V., Allen, M.A., Prausnitz, M.R. (1998). Microfabricated microneedles: a novel approach to transdermal drug delivery. J Pharm Sci. 87:922–5
[5] Donnelly RF, Raj Singh TR, Woolfson AD. Microneedle-based drug delivery systems: microfabrication, drug delivery, and safety. Drug Deliv. 2010;17(4):187-207.
[6] Kern, W. (1978). Chemical etching of silicon, germanium, gallium, arsenide, and gallium phosphide, RCA Rev. 39:278–308.
[7] Metz, T.E., Savage, R.N., Simmons, H.O. (1992). In situ control of photoresist coating process. Semicond Int. 15:68–69.
[8] Justin R, Chen B. Multifunctional chitosan-magnetic graphene quantum dot nanocomposites for the release of therapeutics from detachable and non-detachable biodegradable microneedle arrays. Interface Focus 2018;8(3):20170055.
[9] Apollo NV, Jiang J, Cheung W, Baquier S, Lai A, Mirebedini A, et al. Development and Characterization of a Sucrose Microneedle Neural Electrode Delivery System. Advanced Biosystems 2018;2(2):1700187.
[10] Teo MAL, Shearwood C, Ng KC, Lu J, Moochhala S. In Vitro and In Vivo Characterization of MEMS Microneedles. Biomedical microdevices 2005;7:47-52.
[11] O'Mahony C. Structural characterization and in-vivo reliability evaluation of silicon microneedles. Biomedical microdevices 2014;16(3):333-343.
[12] Ranamukhaarachchi SA, Padeste C, Häfeli UO, Stoeber B, Cadarso VJ. Design considerations of a hollow microneedle-optofluidic biosensing platform incorporating enzyme-linked assays. Journal of Micromechanics and Microengineering 2018;28(2):024002.
[13] Han M, Kim DK, Kang SH, Yoon HR, Kim BY, Lee SS, et al. Improvement in antigen-delivery using fabrication of a grooves-embedded microneedle array. Sensors and Actuators B: Chemical 2008;137:274-280.
[14] Kim JD, Kim M, Yang H, Lee K, Jung H. Droplet-born air blowing: Novel dissolving microneedle fabrication. Journal of Controlled Release 2013;170:430-436.
[15] Kathuria H, Fong MHM, Kang L. Fabrication of photomasks consisting microlenses for the production of polymeric microneedle array. Drug Deliv and Transl Res 2015;5:438-450.
[16] Aggarwal, P., Johnston, C.R. (2004). Geometrical effects in mechanical characterizing of microneedle for biomedical applications. Sens Actuators B. 102:226–234.
[17] Kendall, M.A.F., Chong, Y.F., Alexander, C. (2007). The mechanical properties of the skin epidermis in relation to targeted gene and drug delivery. Biomaterials. 28:4968–4977.

[18] Martanto, W., Davis, S.P., Nicholas, R.H., Wang, J., Gill, H.S., Prausnitz, M.R. (2004). Transdermal delivery of insulin using microneedles in vivo. Pharm Res. 21:947–952
[19] Chang, R.L., Moon, S.K., Lee, H.B., Han, K.L., John, M.R., Gilson, K. (2007). The effect of molecular weight of drugs on transdermal delivery system using microneedle device. Key Eng Mater. 342/3:945–948
[20] Donnelly, R.F., Morrow, D.I.J., Singh, T.R.R., Migalska, K., McCarron, P.A., O'Mahony, C., Woolfson, A.D. (2009a). Processing difficulties and instability of carbohydrate microneedle arrays. Drug Dev Ind Pharm. 35:1242–1254.
[21] Verbaan, F.J., Bal, S.M., van den, D.J.B., Groenink, W.H.H., Verpoorten, H., Lüttge, R., Bouwstra, J.A. (2007). Assembled microneedle arrays enhance the transport of compounds varying over a large range of molecular weight across human dermatomed skin. J Contr Rel. 117:238–245.
[22] Gill, H.S., Prausnitz, M.R. (2007b). Coating formulations for microneedles. Pharm Res. 24:1369–1380.
[23] Xie, Y., Xu, B., Gao, Y. (2005). Controlled transdermal delivery of model drug compounds by MEMS microneedle array. Nanomed Nanotechnol Biol Med. 1:184–190.
[24] Donnelly, R.F., Morrissey, A., McCarron, P.A., Woolfson, D.A. (2007). Microstructured devices for transdermal drug delivery and minimally-invasive patient monitoring. Recent Pat Drug Deliv Formul. 1:195–200.
[25] Jeong, W.L., Park, J.H., Prausnitz, M.R. (2008). Dissolving microneedles for transdermal drug delivery. Biomaterials. 29:2113–124.
[26] Chen, H., Zhu, H., Zheng, J., Mou, D., Wan, J., Zhang, J., Shi, T., Zhao, Y., Xu, H., Yang, X. (2009). Iontophoresis-driven penetration of nanovesicles through microneedle-induced skin microchannels for enhancing transdermal delivery of insulin. J Contr Rel. 139:63–72.
[27] Sivamani, R.K., Stoeber, B., Wu, G.C., Zhai, H., Liepmann, D., Maibach, H. (2005). Clinical microneedle injection of methyl nicotinate: stratum corneum penetration. Skin Res Technol. 11:152–156.
[28] Stoeber, B., Liepmann, D. (2005). Arrays of hollow out-of-plane microneedles for drug delivery. J Microelectromech Syst. 14:472–479.
[29] Damme, P.V., Froukje, O.K., Van der, M.W., Almagor, Y., Sharon, O., Levin, Y. (2009). Safety and efficacy of a novel microneedle device for dose sparing intradermal influenza vaccination in healthy adults. Vaccine. 27:454–459.
[30] Gupta, J., Felner, E.I., Prausnitz, M.R. (2009). Minimally invasive insulin delivery in subjects with type 1 diabetes using hollow microneedles. Diabetes Technol Ther. 11:329–327.